Inorg. Chem. **2005**, *44*, 6463–6469

Three New Phases in the K/Cu/Th/S System: $KCuThS_3$, $K_2Cu_2ThS_4$, and $K_3Cu_3Th_2S_7$

Hugh D. Selby,[†,‡] Benny C. Chan,[†] Ryan F. Hess,[§] Kent D. Abney,[§] and Peter K. Dorhout*[,†]

Department of Chemistry, Colorado State University, Fort Collins, Colorado 80523-1872, Chemistry Division, Los Alamos National Laboratory, Los Alamos, New Mexico 87545, and Nuclear Materials and Technology Division, Los Alamos National Laboratory, Los Alamos, New Mexico 87545

Received April 11, 2005

Synthetic exploration of K/Cu/Th/S quaternary phase space has yielded three new compounds: $KCuThS_3$ (**I**), $K_2Cu_2ThS_4$ (**II**), and $K_3Cu_3Th_2S_7$ (**III**). All three phases are semiconductors with optical band gaps of 2.95, 2.17, and 2.49 eV(**I**–**III**). Compound **I** crystallizes in the orthorhombic space group *Cmcm* with $a = 4.076(1)$ Å, $b = 13.864(4)$ Å, and $c = 10.541(3)$ Å. Compound **II** crystallizes in the monoclinic space group *C*2/*m* with $a = 14.522(1)$ Å, $b = 4.026(3)$ Å, and $c = 7.566(6)$ Å; $\beta = 109.949(1)°$. Compound **III** crystallizes in orthorhombic space group *Pbcn* with $a = 4.051(2)$ Å, $b = 14.023(8)$ Å, and $c = 24.633(13)$ Å. The compounds are all layered materials, with each layer composed of threads of edge-sharing ThS_6 octahedra bridged by CuS_4 tetrahedral threads of varying dimension. The layers are separated by well-ordered potassium ions. The relatively wide range of optical band gaps is attributed to the extent of the CuS_4 motifs. As the dimension of the CuS_4 chains increases, band gaps decrease in the series. All materials were characterized by single-crystal X-ray diffraction, microprobe chemical analysis, and diffuse reflectance spectroscopy (NIR–UV).

Introduction

Recent efforts have been made to explore the solid-state chemistry and physics of materials containing mixed d and f elements. Studies that combine these elements as either dopants in known binary phases or stoichiometric components of novel ternary and quaternary phases have yielded compounds with interesting properties, including heavy fermion behavior, unique magnetic coupling and ordering phenomena, and sensitization and tuning of optical materials.[1−4] Of particular interest are the quaternary lanthanide (Ln) and actinide (An) chalcogenide phases, as the softer chalcogenide (S−Te) components offer diverse bonding modes and a corresponding range of properties not seen in the oxides. The bulk of the exploration thus far has focused on the 4f-nd Ln−transition metal materials, notably the series $CsZnLnSe_3$ (Ln = Sm, Gd−Yb), $CsCdLnSe_3$ (Ln = La−Nd, Sm, Gd−Y), and $CsHgLnSe_3$ (Ln = La−Nd, Sm, Gd−Y), possessing the layered structure type $KCuZrS_3$.[5−8] Many other examples of quaternary Ln−transition metal compounds are known with familiar 2-dimensional layered or pseudo-1-dimensional structures that have incorporated magnetically silent d^{10} coinage metals as the transition metal element.[9−11]

Frequently studied concurrently with the Ln-based materials, the large body of reported early-An-containing analogues

* To whom correspondence should be addressed. E-mail: Peter.Dorhout@colostate.edu. Phone: 970-491-0629. Fax: 970-491-1801.
† Colorado State University.
‡ Chemistry Division, Los Alamos National Laboratory.
§ Nuclear Materials and Technology Division, Los Alamos National Laboratory.

(1) Stewart, G. R. *Rev. Mod. Phys.* **1984**, *56*, 755−787.
(2) Cho, N.; Kikkawa, S.; Kanamaru, F.; Takeda, Y.; Yamamoto, O.; Kido, H.; Hoshikawa, T. *Solid State Ionics* **1993**, *63*−*65*, 696−701.
(3) Murugesan, T.; Ramesh, S.; Gopalakrishnan, J.; Rao, C. N. R. *J. Solid State Chem.* **1981**, *38*, 165−72.
(4) Kageyama, Y.; Oseto, S. Thin-film electroluminescent devices. U.S. Patent 3,712,855, 1988.
(5) Yao, J.; Deng, B.; Sherry, L. J.; McFarland, A. D.; Ellis, D. E.; Van Duyne, R. P.; Ibers, J. A. *Inorg. Chem.* **2004**, *43*, 7735−7740.
(6) Mitchell, K.; Huang F. Q.; McFarland, A. D.; Haynes, C. L.; Somers R., C.; Van Duyne R., P.; Ibers J. A. *Inorg. Chem.* **2003**, *42*, 4109−4116.
(7) Mitchell, K.; Haynes, C. L.; McFarland, A. D.; Van Duyne, R. P.; Ibers, J. A. *Inorg. Chem.* **2002**, *41*, 1199−1204.
(8) Mansuetto, M. F.; Keane, P. M.; Ibers, J. A. *J. Solid State Chem.* **1992**, *101*, 257−264.
(9) Patschke, R.; Heising, J.; Brazis, P.; Kannewurf, C. R.; Kanatzidis, M. *Chem. Mater.* **1998**, *10*, 695−697.
(10) Huang, F. Q.; Choe, W.; Lee, S.; Chu, J. *Chem. Mater.* **1998**, *10*, 1320−1326.
(11) Sutorik, A. C.; Albritton-Thomas, J.; Kannewurf, C. R.; Kanatzidis M. G., *J. Am. Chem. Soc.* **1994**, *116*, 7706−7713.

10.1021/ic050561x CCC: $30.25
Published on Web 08/05/2005

is growing, albeit at a less consistent rate.[12] The introduction of the 5f orbitals has resulted in materials with magnetic behavior not seen in the Ln materials, new structure types, and optical/electronic properties that are consistent with more-diffuse f electrons.[13,14] Because of the special handling requirements associated with the elements Ac, Pa, Np, and Pu, most of the reported materials feature Th and U as the An component, with U by far the most thoroughly explored. Thorium has been neglected largely because of its strong thermodynamic preference for the Th(IV) f^0 state, which is less interesting from the perspective of magnetic or electronic studies than the U(IV) f^2 equivalent. Moreover, Th(IV) compounds are often isostructural with their U(IV) analogues. We wish to report here three new Th-containing quaternary phases which, to the best of our knowledge, have no compositional U analogues. The phases $KCuThS_3$ (**I**), $K_2Cu_2ThS_4$ (**II**), and $K_3Cu_3Th_2S_7$ (**III**) are semiconductors with striking variations in color and range of measured band gaps, despite quite similar compositions and closely related structures.

Experimental Section

Caution: *^{232}Th is a naturally occurring radioisotope which decays by α-emission ($t_{1/2} = 1.4 \times 10^{10}$ years) and should be handled only in radiological areas.*

Synthesis. All reagents were used as received and stored in an inert (N_2)-atmosphere glovebox: Th (metal foil, c.a. 99.9%, Los Alamos National Laboratory), S (99.999%, Johnson-Mathey), K (99.999%, Aldrich), and Cu (99.99% Fisher Scientific). All reactions were performed in a K_2S_2 molten flux, which was prepared by stoichiometric reaction of the elements in liquid ammonia per literature methods.[15] Reagents were loaded into fused silica ampules inside the storage glovebox. The ampules were removed from the glovebox, flame-sealed under vacuum, and placed in a temperature-controlled tube furnace. The furnace was then heated to 500 °C at 35°/h and held at that temperature for 288 h. Reactions were slowly cooled to ambient temperature at 5°/h. Products of interest were separated from the unreacted salt flux by repeatedly washing the sample with *N*,*N*′-dimethylformamide (DMF) until the supernatant was clear (the excess solvated K_xS_y flux is an intense blue color). All products were air stable indefinitely. Randomly selected crystals diffracted with comparable intensity and quality to the originals after exposure to air for periods of weeks to months. In all cases, the compounds were not targeted by stoichiometric combination but were discovered as a part of the exploration of quaternary phase space (K/Th/Cu/S). Compositions of the title compounds, as determined by energy-dispersive X-ray analyses (EDS) on a JEOL 6300 SEM, were therefore not necessarily related to the stoichiometry of the reactions. Errors in this method are ca. ±5%.

Compound **I** was synthesized by reacting 58.3 mg (0.251 mmol) of Th, 129.3 mg (2.030 mmol) of Cu, 65.1 mg (2.03 mmol) of S, and 34.3 mg (0.241 mmol) of K_2S_2. Following washing by DMF, the sample contained a mixture of colorless rod/plate crystals of **I**, the metallic green ternary KCu_4S_3, and the metallic purple covellite phase of the mineral CuS (both identified by single-crystal cell parameters).[16,17] Compound **I** was the minor component of the mixture, at approximately 25% of the bulk. EDS analysis of selected single crystals of **I** revealed the following composition normalized to Th: $K_{0.833}Cu_{1.05}ThS_{2.37}$.

Compound **II** was synthesized by reacting 86.9 mg (0.375 mmol) of Th, 24.7 mg (0.389 mmol) of Cu, 24.0 mg (0.748 mmol) of S, and 71.3 mg (0.501 mmol) of K_2S_2. Thorough DMF washing left a mixture of a small amount of unreacted Th metal, a passivating layer of **II** on the Th metal, and a few fibrous, green crystals of KCu_3S_2 (identified by single-crystal unit cell parameters).[18] The major product comprised red, irregularly shaped crystals of **II**, forming approximately 80% of the bulk. Atomic composition of **II** was found by EDS to be $K_{2.45}Cu_{2.45}ThS_{5.14}$, normalized to Th. Crystals of **II** were intimately mixed with small amounts of elemental S, which likely contributed to the relative abundance of S in the chemical analysis.

Compound **III** was synthesized by reacting 29.3 mg (0.126 mmol) of Th, 47.3 mg (0.744 mmol) of Cu, 128.7 mg (4.013 mmol) of S, and 283.0 mg (1.987 mmol) of K_2S_2. Repeated DMF washing revealed a mixture that, by visual inspection, was approximately 60% **III** and 40% KCu_4S_3 (determined by single-crystal cell parameters).[16] No other products were observed. Compound **III** crystallized as very thin, yellow plates that grew in clusters. A few of these clusters were analyzed by EDS to yield the atomic composition $K_{1.59}Cu_{1.59}ThS_{3.84}$, normalized to Th.

It is of note that compound **I** could be prepared in near quantitative yield by stoichiometric combination using K_2S_2 as the sulfur source under otherwise identical conditions. However, **II** and **III** could not be made pure via the low-temperature route; significant quantities of binary and ternary thiocuprate phases were always present. Even lower temperatures (480 °C, K_2S_2; 270 °C, K_2S_5) served only to enhance the amount of the thiocuprate phases formed. This observation suggests that the mobility of the Cu(I) ion couples with the high relative stability of the binary and ternary phases to create a readily accessible thermodynamic sink. Elevated-temperature experiments are in progress to determine if **II** and **III** may be isolated as pure phases.

Single-Crystal X-Ray Diffraction. Suitable single crystals of **I**, **II**, and **III** were coated with epoxy and mounted to glass fibers in random orientations. The crystals were then mounted on a Bruker SMART 1000 CCD-equipped diffractometer. Intensity data were collected at room temperature using the graphite-monochromated Mo Kα line collimated to 0.5 mm. Three sets of 606 0.3°-wide frames were obtained at three settings of φ (0°, 120°, 240°) as ω-scans. An additional set of 50 frames collected at the initial φ,ω settings revealed no measurable decay. Exposure times for **I** and **II** were 20 s; they were 30 s for **III**. Additional data for **III** were collected on a Bruker APEXII diffractometer using an identical scan program but with 15 s frames. The data for **III** indicated that the sample was cracked or composed of closely aligned crystallites (several reflections broader than 1° in ω; an additional weak lattice that could be indexed to that of **III**). Constraining the integration to the dominant lattice afforded intensity data of quality sufficient for reasonable structural solution. Cell parameters for integration were determined from the full data sets, and integration was performed using SAINT.[19] Structures were solved with direct

(12) Narducci, A. A.; Ibers, J. A. *Chem. Mater.* **1998**, *10*, 2811−2823.
(13) Choi, K.-S.; Iordanidis, L.; Chondroudis, K.; Kanatzidis, M. G. *Inorg. Chem.* **1997**, *36*, 3804−3805.
(14) Choi, K.-S.; Patschke, R.; Billinge, S. J. L.; Waner, M. J.; Dantus, M.; Kanatzidis, M. G. *J. Am. Chem. Soc.* **1998**, *120*, 10706−10714.
(15) Sunshine, S. A.; Kang, D.; Ibers, J. A. *J. Am. Chem. Soc.* **1987**, *109*, 6202−4.
(16) Ruedorff, W.; Schwarz, H. G.; Walter, M. *Z. Anorg. Allg. Chem.* **1952**, *269*, 141−152.
(17) Roberts, H. S.; Ksanda, C. J. *Am. J. Sci.* **1929**, *17*, 489−503.
(18) Burschka, C.; Bronger, W. *Z. Naturforsch. B* **1977**, *32*, 11−14.
(19) *SAINT.; Data processing software for the SMART system*; Bruker Analytical X-ray Instruments, Inc.: Madison, WI, 1995.

Table 1. Crystallographic Data for **I**, **II**, and **III**

empirical formula	$KCuThS_3$ (**I**)	$K_2Cu_2ThS_4$ (**II**)	$K_3Cu_3Th_2S_7$ (**III**)
fw	430.86	565.56	996.42
a, Å	4.076(1)	14.522(1)	4.051(2)
b, Å	13.864(4)	4.026(3)	14.023(8)
c, Å	10.541(3)	7.566(6)	24.633(1)
α, deg	90.00	90.00	90.00
β, deg	90.00	109.949(1)	90.00
γ, deg	90.00	90.00	90.00
V, Å^3	595.7(3)	415.8(5)	1399.4(1)
Z	4	2	4
λ(Mo Kα), Å	0.71073	0.71073	0.71073
space group	*Cmcm* (No.63)	*C*2/*m* (No.12)	*Pbcn* (No.60)
temp., K	298(2)	298(2)	298(2)
$\rho_{calc.}$, Mg/m^3	4.804	4.517	4.729
R1%[a]	0.0236	0.0337	0.0785
wR2%[a]	0.0495	0.0708	0.2169

[a] $R1 = \sum(|F_o| - |F_c|)/\sum|F_o|$; $wR2 = [\sum[w(F_o^2 - F_c^2)^2]/\sum[w(F_o^2)^2]]^{1/2}$.

Table 2. Selected Bond Distances (Å) for $KCuThS_3$ (**I**)

bond	distance (Å)
Th(1)−S(1) (2 eqiv)	2.7872(2)
Th(1)−S(2) (4 eqiv)	2.7838(5)
Cu(1)−S(1) (2 eqiv)	2.455(2)
Cu(1)−S(2) (2 eqiv)	2.334(2)
K(1)−S(1) (2 eqiv)	3.197(3)
K(1)−S(2) (4 eqiv)	3.338(3)
K(1)−S(2)a (2 eqiv)	3.700(6)

Table 3. Selected Bond Distances (Å) for $K_2Cu_2ThS_4$ (**II**)

bond	distance (Å)
Th(1)−S(1) (4 eqiv)	2.794(2)
Th(1)−S(2) (2 eqiv)	2.781(3)
Cu(1)−S(1)	2.378(3)
Cu(1)−S(2)	2.425(2)
Cu(1)−S(2)a	2.429(3)
K(1)−S(1) (2eqiv)	3.401(3)
K(1)−S(1)a (2eqiv)	3.296(4)
K(1)−S(2) (2eqiv)	3.185(3)
K(1)−S(2)a	3.364(5)

Table 4. Selected Bond Distances (Å) for $K_3Cu_3Th_2S_7$ (**III**)

bond	distance (Å)	bond	distance (Å)
Th(1)−S(1)	2.79(2)	Cu(2)−S(2) (2 eqiv)	2.333(6)
Th(1)−S(2)	2.75(2)	Cu(2)−S(4) (2 eqiv)	2.422(5)
Th(1)−S(3)	2.793(6)	K(1)−S(1) (2 eqiv)	3.546(7)
Th(1)−S(4)	2.803(3)	K(1)−S(2) (2 eqiv)	3.35(2)
Th(1)−S(1)a	2.76(2)	K(1)−S(2)a (2 eqiv)	3.40(2)
Th(1)−S(2)a	2.82(2)	K(1)−S(4) (2 eqiv)	3.185(8)
Cu(1)−S(1)	2.351(7)	K(2)−S(1)	3.11(2)
Cu(1)−S(3)	2.43(3)	K(1)−S(1)a	3.13(2)
Cu(1)−S(3)a	2.472(7)	K(1)−S(2)	3.139(8)
Cu(1)−S(3)b	2.47(3)	K(1)−S(3)	3.31(3)

methods and refined using the XS and XL components of the SHELXTL software suite.[20] A SADABS absorption correction was applied to all data sets.[21] Additional details are reported for **I**, **II**, and **III** in Table 1, and CIF files for all three are available as Supporting Information. Selected bond lengths are included in Tables 2−4.

UV−Visible Spectroscopy. Samples were manually separated from their mixtures and gently ground to uniform microcrystalline powders. These samples were analyzed using a Varian Cary 500 Scan UV−vis−NIR spectrophotometer fitted with a Praying Mantis accessory. A Teflon standard was used as a reference. Data were treated with the Kubelka−Munk function, and the extrapolation method was used to determine the band gaps.[22, 23]

Results and Discussion

Structural Results. Compound **I** crystallized in the orthorhombic space group *Cmcm*. Likely the result of its remarkable stability, excellent quality crystals of **I** could be obtained in high purity from a range of compositions.[24] Consequently, the structural model was straightforward. All atoms were given anisotropic thermal parameters, and a full matrix, least-squares refinement converged to a final R1 of 2.36%. No evidence of disorder or twinning was discovered. Compound **I** has two crystallographically unique sulfur atoms with S−Th and S−Cu distances of 2.7872(2)−2.7838(5) Å and of 2.334(2)−2.455(2) Å, respectively. These distances are consonant with the formal oxidation states of Th(IV), Cu(I), and S^{2-} making **I** electron precise and a likely insulator or semiconductor. Compound **I** is a member of the large family of quaternary phases, $AMRQ_3$ (A = alkaline metal; M = transition metal; R = Ln, An metal; Q = chalcogenide), with the $KCuZrS_3$ structure type. The structure consists of sheets that stack in the [010] direction, separated by well-ordered potassium cations. To use a textile analogy, the sheets are woven from alternating threads of ThS_6 octahedra and CuS_4 tetrahedra which run in the [100] direction. ThS_6 threads are formed by equatorial sulfur atoms that are edge sharing and linked to the CuS_4 tetrahedra by one axial and one equatorial S atom. The CuS_4 threads are formed by corner-sharing of an apical sulfur atom contributed by the ThS_6 octahedra. The sheets are corrugated by virtue of glide symmetry, making the sense of every other CuS_4 tetrahedral threads opposed. The Cu sites from thread to thread are alternating above and below the plane of thorium atoms. The ThS_6 octahedra are likewise opposed within a given sheet. The sheets are anionic and may be described in the shorthand empirical form as $^2_\infty[CuThS_3^-]$. Figure 1 shows the sheets with their charge-balancing potassium cations in the interlayer gallery.

As previously noted, this structure is related to a number of ternary compounds: $MAnQ_3$, including $FeUS_3$ and the more compositionally relevant $MnThSe_3$.[25,26] These two ternary phases feature distinct sheets with the same parent MQ_6 octahedral threads forming the sheets as in **I**. However, in these other phases, sites that would be equivalent to our Cu T_d sites are empty and the transition elements exert their strong size and electronic preferences for the octahedral sites. In the $MAnQ_3$ phases, the An element occupies what would be the larger 'A' sites in **I** and create an overall structure that is an extended 3D array. Consideration of the anionic sheet formulation $^2_\infty[CuThS_3^-]$ leads one to the $NaLnQ_3$ class

(20) *SHELXTL 6.10*; Brukers AXS, Inc.: Madison, WI, 2000.
(21) Sheldrick, G. M. *SADABS*; University of Gottingen: Gottingen, Germany, 1997.
(22) McCarthy, T.; Ngeyi, S.-P.; Liao, J.-H.; DeGroot, D. C.; Hogan, T.; Kannewurf, C. R.; Kanatzidis, M. G. *Chem. Mater.* **1993**, *5*, 331−340.
(23) Wilkinson, F.; Kelly, G. In *CRC Handbook of Organic Photochemistry*; Scaiano, J. C. CRC Press: Boca Raton, FL, 1989; Vol. 1, 293−314.
(24) Sutorik, A. C.; Albritton-Thomas, J.; Hogan, T.; Kannewurf, C. R.; Kanatzidis, M. G. *Chem. Mater.* **1996**, *8*, 751−761.
(25) Noel, H.; Padiou, J. *Acta Crystallogr. B* **1976**, *32*, 1593−1595.
(26) Narducci, A. A.; Ibers, J. A. *Inorg. Chem.* **2000**, *39*, 688−691.

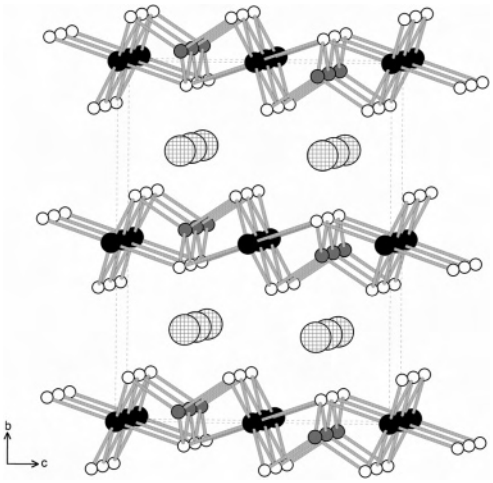

Figure 1. Packing diagram of **I**, showing corrugated sheets consisting of ThS_6 octahedra and CuS_4 tetrahedra: crosshatched spheres = K^+; black spheres = Th(IV); gray spheres = Cu(I); hollow spheres = S^{2-}.

of compounds which, with the parent $ZrSe_3$ structure, are not obviously related to **I**.[27] Yet, with some manipulation of the subtle interplay of redox chemistry and the thermodynamic need to minimize structural voids, a relationship can be developed.

For example, to make the charge balance in $ZrSe_3$, some of the selenides are oxidized to form Se_2^{2-} anions. These diselenide units form the alternating tops and bottoms of the $ZrSe_3$ sheets, with the Zr atoms in distorted bicapped trigonal prismatic sites. The Se_2^{2-} units are considerably larger than a single selenide anion and serve to take up the large void volume that would result from such a charge-allowed substitution. Like the ThS_6 octahedra of **I**, the Zr prisms form threads, in this instance by face sharing. Each of the diselenide units bridges the Zr atoms in a given thread and are bound normal to the thread direction in a $\mu-\eta^2$ fashion. Because of the bridging interaction, the diselenide units are shared between neighboring Zr atoms and are equivalent by stoichiometry to two single-selenide anions per Zr atom. Alternatively, one could consider the η^2 binding mode as occupying a single large coordination site (akin to an olefin complex) and one would still arrive at a single selenide anion equivalent per Zr atom. From either perspective, the coordination number of Zr could be argued to be 6, not 8. Such an argument suggests the trigonal prismatic coordination in $ZrSe_3$ hides an octahedron and creates a link to the MQ_6 octahedra in $MnThSe_3$ and **I**.

With this notion in mind, one may perform the *gedanken* experiment shown in Figure 2. If the two diselenide units are simply condensed to a single site at the Se−Se centroid, the Zr coordination environment becomes a grossly distorted octahedron with large voids in the lattice. Note that the bridging interaction of the new artificial monoselenide interaction is maintained and the distorted octahedra are now edge sharing as in **I**. The distortion is now contained in the axial Se−M−Se bend. If this imaginary structure is allowed to relax and 1 equiv of $ZrSe_2$ per cell is removed (the top or bottom half of the $ZrSe_3$ sheet may be thought of as having an extra O_h site filled with respect to **I**), it becomes isostructural with the anionic layers in $MnThSe_3$. Indeed, the imaginary stoichiometry is maintained in dianionic sheets that may be written as $^2_\infty[ZrSe_3^{2-}]$. Void-filling and charge balance are then trivial matters of placing the appropriate atoms in the correct sites to re-create a structure related to compound **I**. If $ZrSe_3$ is not considered the parent structure, one may consider it to be a "close uncle" structure, and this suggests a range of unexplored variations within the three canonical structure types $ZrSe_3$, $MAnQ_3$, and $AMRQ_3$.

Compound **II** crystallized in the space group *C*2/*m*. The final R1 value for a full matrix, least-squares refinement with all atoms treated anisotropically converged at 3.337%. A rendering of **II** can be seen in Figure 3.

Compound **II** also features a layered structure with a close relationship to **I**. In **II**, the sheets are similarly composed of alternating threads of edge-sharing ThS_6 octahedra and CuS_4 tetrahedra with potassium cations in the interlayer gallery. However, the ThS_6 threads are separated completely from each other in the sheet by a double thread of edge-sharing CuS_4 tetrahedra as shown in Figure 3. In contrast, the threads of ThS_6 in **I** share vertexes in the direction normal to their direction of propagation. At first glance, the sheets in **I** and **II** appear to be virtually identical, save for the extra CuS_4 thread in **II**. Upon examination of the layers in **II**, one finds that the edge-sharing CuS_4 tetrahedra are related by a pseudo-inversion center. This has the effect of orienting the octahedra in the same direction within the sheet, eliminating the corrugation observed in **I**.

The structure of **II** is remarkably rare, with only one known Ce-containing analogue, $K_2Cu_2CeS_4$.[24] This Ce structure and that of compound **II** are closely related to the magnesium−silicate mineral olivine and share an interesting relationship with $FeTaTe_3$.[28,29] In the latter material, each sheet is composed of a 2 (octahedra):1 (tetraheda) thread pattern ratio. This is the opposite ratio of that observed in **II**, with the $TaTe_6$ octahedral threads being doubled with only single $FeTe_4$ tetrahedral threads separating them. It is also possible to relate compound **II** to CdI_2 when considering the distorted *hcp* lattice of sulfur atoms in a given layer of **II**. Instead of every octahedral hole being filled, as in CdI_2, every third octahedral hole is filled in **II**. Like compound **I**, bond lengths lead to an assignment of formal oxidation states, Th(IV), Cu(I), and S^{2-}, and precise electron count.

Unfortunately, only single crystals of moderate to poor quality (R1 = 7.85%) could be found for **III**. However, a dataset did provide enough information to confidently assign atomic positions on the basis of relative peak heights and reasonable bond length and angle measurements. The structure could be solved in several space groups; each gave the same model. Also, crystal morphology and color were distinct from compounds **I** and **II** and the absorption edge is shifted significantly from **I** and **II**. Finally, the microprobe analysis was in excellent agreement with the composition

(27) Sutorik, A. C.; Kanatzidis, M. G. *Chem. Mater.* **1997**, *9*, 387−398.

(28) Carpenter, J. D.; Hwu, S. J. *Chem. Mater.* **1992**, *4*, 1368−1372.

(29) Liu, S.-X.; Cai, G.-L.; Huang, J.-L. *Acta Crystallogr. C* **1993**, *49*, 4−7.

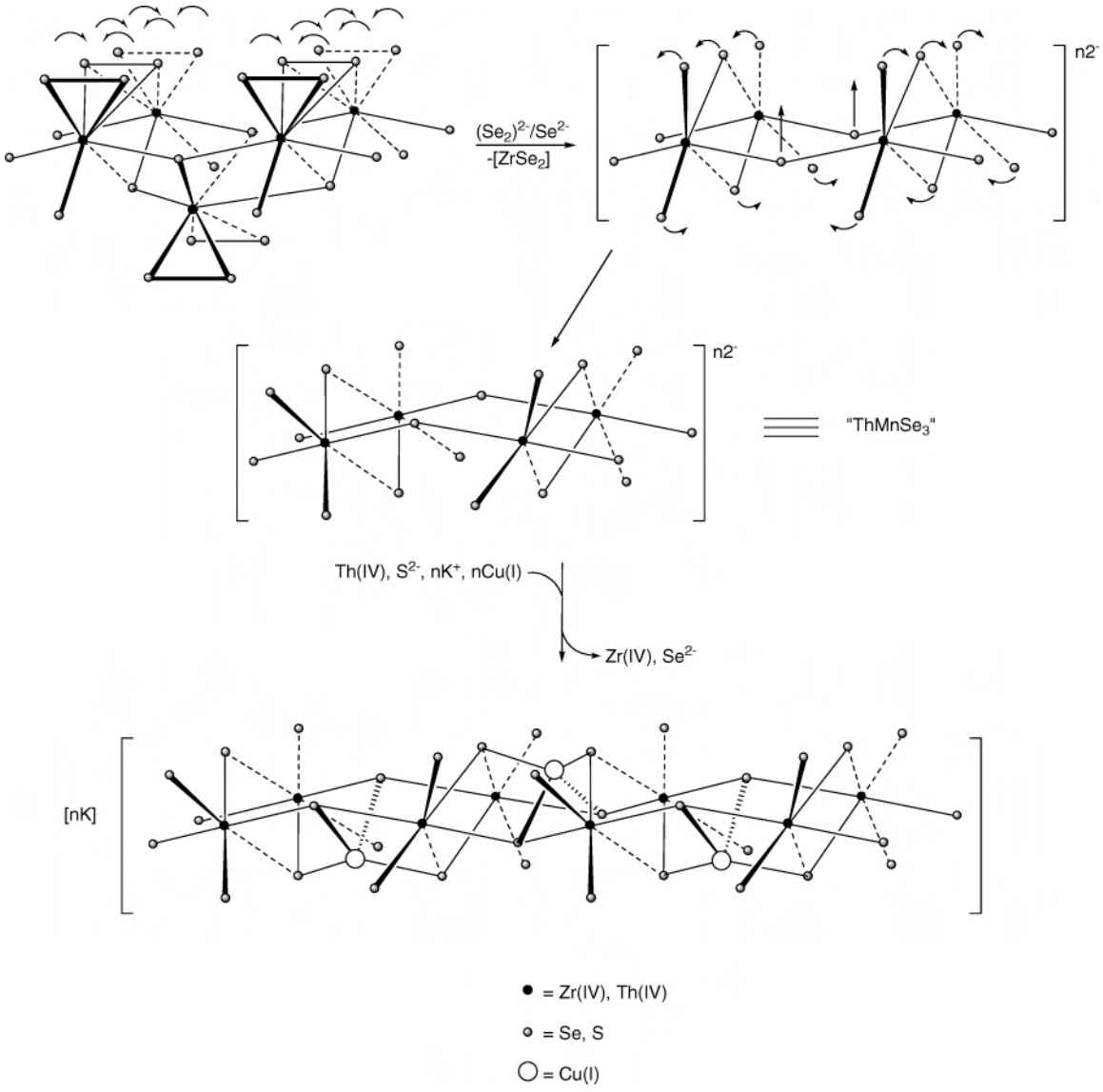

Figure 2. The pseudo-synthetic relationship between $ZrSe_3$ and **I**.

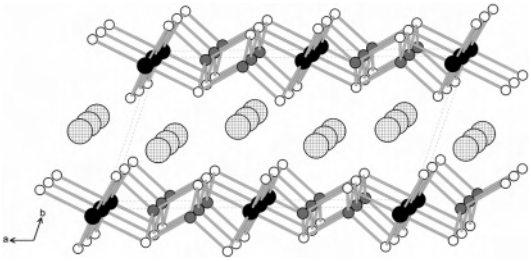

Figure 3. Packing diagram of **II**, formed from sheets of ThS_6 octahedra and doubled CuS_4 tetrahedra: crosshatched spheres = K^+; black spheres = Th(IV); gray spheres = Cu(I); hollow spheres = S^{2-}.

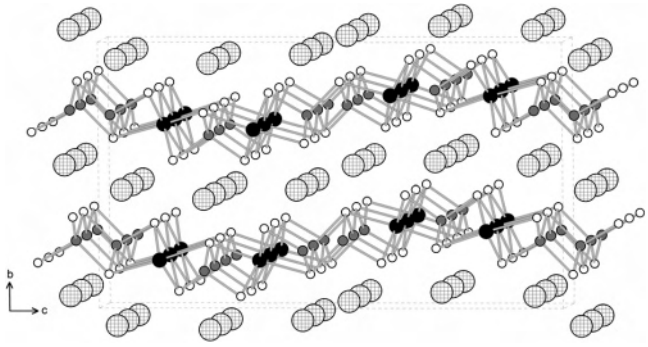

Figure 4. Packing diagram of **III**, featuring a sinusoidal distortion of the sheets as a result of the combination of both single and double CuS_4 threads linking the ThS_6 octahedra: crosshatched spheres = K^+; black spheres = Th(IV); gray spheres = Cu(I); hollow spheres = S^{2-}.

derived from the structure. These three observations led us to conclude that the reported model is reasonable and correct. The final structure was solved by direct methods in the space group *Pbcn*. This was the most reasonable choice on the basis of systematic absences, manual examination of reciprocal space symmetry, and quality of refinement. Atomic positions were readily located, but high residual electron density remained near S1. This peak was also close to Cu1 and K2 and modeled reasonably well as a partially occupied S site. However, the proximity to the other sites was chemically unreasonable in addition to violating the logical as-found stoichiometry. Efforts to refine the structure as a simple twin did not improve the situation, and the data were insufficient to model with confidence nonmerohedral twins. Analysis of

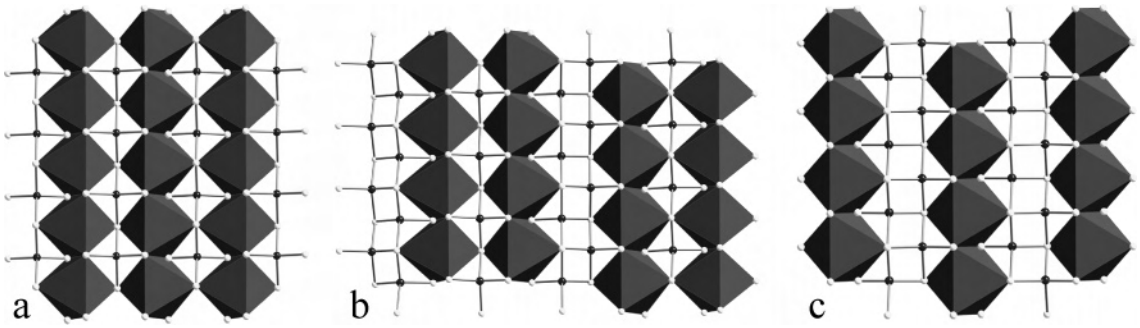

Figure 5. A comparison of the three sheet types and progression of the CuS_4 dimensionality for **I**−**III**: a = **I**, b = **III**, c = **II**; octahedra = Th(IV), gray spheres = Cu(I); colorless spheres = S^{2-}.

the raw data revealed a number of weak reflections that did not fit the cell well, which suggested the presence of closely aligned crystallites or cracking. This was corroborated by the observation of striations along the major axis of the macroscopic crystal. Despite constraints placed on the integration, the resultant data did not allow for reliable application of sophisticated disorder/twin models. We therefore concluded that the high residual density was an artifact of poor data. All other sites were refined isotropically.

Compound **III** has a layered structure much like those of **I** and **II**. In fact, the structure is an interesting hybrid of compounds **I** and **II**. Like **I** and **II**, the sheets are composed of alternating threads of ThS_6 octahedra linked by CuS_4 tetrahedra, with potassium ions between the sheets. Again, single threads of ThS_6 octahedra are formed by edge sharing, extending in the [100] direction. Instead of only single or only double CuS_4 threads joining the ThS_6 threads, compound **III** features both. On one side of the ThS_6 octahedral thread is a single CuS_4 thread like those found in compound **I**, on the other, a double thread similar to compound **II**. This combined pattern results in the sheets exhibiting a sinusoidal distortion from planarity that propagates along [001] as shown in Figure 4. Figure 5 shows a comparison of the thread patterns in compounds **I**−**III**. This comparison reveals the relationship between the three structures: The structure of **III** may be considered to be an intermediate between the 1:1 octahedron/tetrahedron ratio of **I** and the 1:2 ratio found in **II**. This interpretation is supported by the analysis of the empirical formulas of the three compounds. Compound **I** has a 1:1:1:3 ratio of K, Cu, Th, and S, respectively. Compound **II** has the ratio 2:2:1:4, and **III**'s ratio is 3:3:2:7 or 1.5:1.5:1:3.5. This fractional composition is exactly between **I** and **II**. Like **I** and **II**, the empirical formula and reasonable bond lengths make **III** electron precise with formal oxidation states of Th(IV), Cu(I), and S^{2-}. To the best of our knowledge, **III** is a new structure type.

Optical Band Gap Measurements. The diffuse reflectance data for **I**−**III** are shown in Figure 6. The band gaps were 2.95, 2.17, and 2.49 eV for **I**, **II**, and **III**, respectively. As expected from the precisely determined oxidation states, the measured band gaps for all three phases fall in the normal range for semiconductors. However, two significant differences exist between the three samples. The most obvious difference is the relatively wide spread of band gaps within the series—nearly an electronvolt for seemingly small differences in structure. The other difference is appearance of complicated structure at the onset of absorption for **II** and **III**, in contrast with the very sharp absorption edge for **I**.

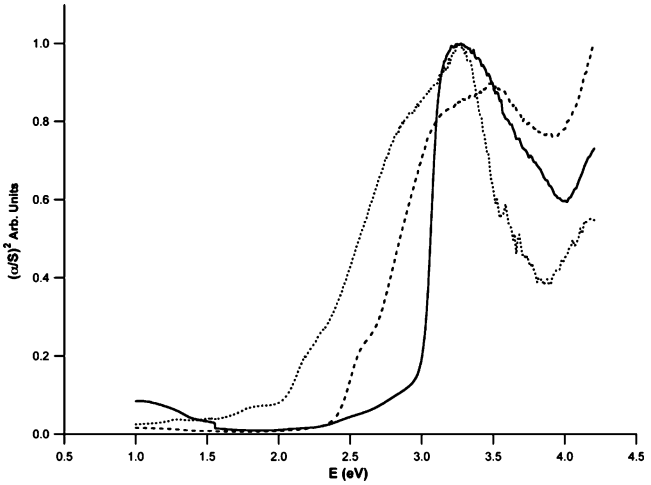

Figure 6. Diffuse reflectance spectra of **I**−**III** {— (**I**), ····· (**II**), - - - - (**III**)}.

Several recent papers have discussed the nature of the observed band gaps in layered materials similar to the title compounds.[5,7,30−32] The conclusion reached by the authors of these articles was that the band gap was primarily a function of 1) the distance between the layers and the corresponding degree of interlayer van der Waals contact and 2) the dimensionality of features within a layer and their relative covalency. Since the title compounds all have potassium cations in the interlayer gallery, there is no true van der Waals gap and the distance between layers is not likely a factor in determing the optical band gap. The second effect, however, is quite likely to have a strong influence on the value of the optical gap. Extensive calculations on Ln/d^{10} compounds isostructural with **I** have shown that the materials are direct band gap semiconductors with narrow bands due to the primarily ionic interactions between the metals and the chalcogenide anions.[6] Since the title compounds contain f^0 Th(IV), we propose that the Th frontier orbitals are noninteracting and high-lying components of the conduction band, leaving the Cu 3d and S 3p states

(30) Huang, F. Q.; Ibers, J. A. *Inorg. Chem.* **2001**, *40*, 2602−2607.
(31) Axtell, E. A., III.; Park, Y.; Chondroudis, K.; Kanatzidis, M. G. *J. Am. Chem. Soc.* **1998**, *120*, 124−136.
(32) Brown, D. B.; Zubieta, J. A.; Vella, P. A.; Wrobleski, J. T.; Watt, T.; Hatfield, W.; Day, P. *Inorg. Chem.* **1980**, *19*, 1945−1950.

contributing most to the direct band gap, akin to the aforementioned Ln materials and the $A_2TiM_2S_4$ (A = Rb, Cs; M = Cu, Ag) series.[30] The presence of Th sites in the otherwise contiguous CuS_4 framework serves to break up the extended Cu−S interactions, reducing them to pseudo-1D and narrow 2D interactions in the title compounds. As discussed in other systems, this reduction in dimensionality decreases the number of close-lying Cu−S states and narrows and separates the bands.[31] Applying this logic allows us to explain the shifts in absorption across the series **I**−**III**. Compound **I** has only a single thread of CuS_4 tetrahedra and therefore the least diffuse bands and largest band gap. Compound **II** features double CuS_4 threads with more extended Cu−S interaction leading to the most diffuse bands and the narrowest band gap. Since **III** has both types of threads in isolation, its absorbance profile would appear to be the superposition of **I** and **II**. Further theoretical investigation is required to confirm this hypothesis.

The second feature of the spectra, the complicated structure observed in **II** and **III**, is less easily rationalized. Compound **I** is a direct analogue for the $CsMLnSe_3$ materials and, like them, is clearly a simple direct band gap semiconductor. The pre-gap structure in **II** and **III** could be the result of impurity, but the impurities in both compounds do not have bands in the region in question.[32−34] It is more likely that the features are intrinsic to the materials and suggests indirect transitions and complex band structure. It is imprudent to speculate what gives rise to these bands without the benefit of theoretical computation. However, **II** and **III** both have larger numbers of crystallographically unique S and Cu atoms and/or lower symmetry than **I** and may consequently have larger numbers of energetically discrete states close to the Fermi level.

Conclusion

The successful synthesis and characterization of $KCuThS_3$, $K_2Cu_2ThS_4$, and $K_3Cu_3Th_2S_7$ marks the first entry in the K/Cu/Th/S phase diagram. Although the first two compounds do have analogues in other compositions, none are known in the present system.[24,35] The third compound, $K_3Cu_3Th_2S_7$, appears to be a structural and spectroscopic hybrid of the first two and may represent a new structure type. More significantly, each of these materials exhibits characteristic optical band gaps that are quite well separated from each other. This observation is related to the extent of the CuS_4 network featured in each structure, suggesting that Th concentration is the synthetic handle for tuning the optical properties of related materials. To date, these materials have no reported U analogues, although work in this direction is proceeding. Even though the U analogues are all likely isolable, the title compounds remain important because they provide understanding of electronic structure in the absence of complicating f electrons. Such a basis will allow for a more certain structure/function relationship to be developed once the magnetic U analogues are in hand.

Acknowledgment. The authors thank Ms. Susie Miller and Dr. Brian Scott for the use of their X-ray diffractometers and Dr. Sandeep Kholi for training on the diffuse reflectance instruments. Funding for this work was provided by the Department of Energy, Heavy Element Chemistry-ER15351 and the NMT division of Los Alamos National Laboratory (H.D.S.).

Supporting Information Available: Additional crystallographic details in CIF format. This material is available free of charge via the Internet at http://pubs.acs.org.

IC050561X

(33) Folmer, J. C. W.; Jellinek, F. *J. Less-Common Met.* **1980**, *76*, 153−162.
(34) Peplinski, Z.; Brown, D. B.; Watt, T.; Hatfield, W.; Day, P. *Inorg. Chem.* **1982**, *21*, 1752−1755.
(35) Cody, J. A.; Ibers, J. A. *Inorg. Chem.* **1995**, *34*, 3165−3172.